Available online at www.sciencedirect.com
SCIENCE DIRECT®
Journal of Environmental Radioactivity 89 (2006) 18–29
JOURNAL OF ENVIRONMENTAL RADIOACTIVITY
www.elsevier.com/locate/jenvrad

Absorbed dose in target cell nuclei and dose conversion coefficient of radon progeny in the human lung

D. Nikezic [a,b], B.M.F. Lau [a], N. Stevanovic [b], K.N. Yu [a,*]

[a] *Department of Physics and Materials Science, City University of Hong Kong, Tat Chee Avenue, Kowloon Tong, Hong Kong*
[b] *Faculty of Science, University of Kragujevac R. Domanovic 12, 34000 Kragujevac, Serbia and Montenegro*

Received 12 October 2005; received in revised form 8 January 2006; accepted 8 March 2006
Available online 5 May 2006

Abstract

To calculate the absorbed dose in the human lung due to inhaled radon progeny, ICRP focussed on the layers containing the target cells, i.e., the basal and secretory cells. Such an approach did not consider details of the sensitive cells in the layers. The present work uses the microdosimetric approach and determines the absorbed alpha-particle energy in non-spherical nuclei of target cells (basal and secretory cells). The absorbed energy for alpha particles emitted by radon progeny in the human respiratory tract was calculated in basal- and secretory-cell nuclei, assuming conical and ellipsoidal forms for these cells. Distributions of specific energy for different combinations of alpha-particle sources, energies and targets are calculated and shown. The dose conversion coefficient for radon progeny is reduced for about 2 mSv/WLM when conical and ellipsoidal cell nuclei are considered instead of the layers. While changes in the geometry of secretory-cell nuclei do not have significant effects on their absorbed dose, changes from spherical to conical basal-cell nuclei have significantly reduced their absorbed dose from ~4 to ~3 mGy/WLM. This is expected because basal cells are situated close to the end of the range of 6 MeV alpha particles. This also underlines the significance of better and more precise information on targets in the T-B tree. A further change in the dose conversion coefficient can be achieved if a different

* Corresponding author. Tel.: +852 2788 7812; fax:+852 2788 7830.
E-mail address: appetery@cityu.edu.hk (K.N. Yu).

0265-931X/$ - see front matter
doi:10.1016/j.jenvrad.2006.03.001

weighting scheme is adopted for the doses for the cells. The results demonstrate the necessity for better information on the target cells for more accurate dosimetry for radon progeny.

Keywords: Radon progeny; Dosimetry; Dose conversion coefficient

1. Introduction

To calculate the absorbed dose in the human lung due to inhaled radon progeny, ICRP66 (ICRP, 1994) made use of the absorbed fraction (AF) which is the average energy of alpha particles absorbed in layers containing the target cells. The AF for a given combination of a source and a target has to be multiplied with the number of alpha particles emitted in that source to give the energy absorbed in the target. ICRP66 considered the layers containing the target cells, i.e., the basal and secretory cells. Such an approach did not consider the structure, orientation, shape and abundance distribution of the sensitive cells in the layers. Furthermore, in the weighting procedure, the basal and secretory cells were assumed equally sensitive to alpha particles. Moreover, the absorbed doses in the bronchial (BB) region (generations 1–8) and in the bronchiolar (bb) region (generations 9–15) of the human lung were assumed to have the same weighting factor of 0.333, although the numbers of cancer appearance are different in these two regions (ICRP, 1994).

Nikezic and Yu (2001) replaced calculations of the absorbed energy in the layers by calculations of the absorbed energy in spherical cell nuclei. Hofmann et al. (2004) also used spherical cell nuclei to calculate the LET spectra for radon progeny under the bifurcation and cylindrical geometry and to study the effects of non-uniform deposition of radon progeny on the absorbed dose. However, in reality, basal and secretory cells are not spherical, and in fact can be far from spherical. Usually, the cell nucleus ''follows'' the shape of the cell itself. Basal cells are close to irregular cones while secretory cells are close to ellipsoids. In this way, there is a reason to assume that the cell nuclei are not spherical. In particular, basal cells are situated close to the end of the range of 6 MeV alpha particles so their geometry might significantly affect the received dose. The main objective of the present study is to investigate the effects of the geometry of basal and secretory cells on the microdosimetric parameters and distribution, as well as on the absorbed dose received by the nuclei of these cells.

By focusing on the absorbed energy in spherical cell nuclei, Nikezic and Yu (2001) obtained the dose conversion coefficient (DCC) of 10 mSv/WLM. In that work, calculations were performed for airway tubes with a length of 2 mm (Nikezic and Yu, 2001). Subsequently, we found that the absorbed fraction would increase with the tube length due to the influence of the opposite (far) wall of the tube in calculations (Nikezic et al., 2003) and saturation was achieved for the tube length of about 2 cm. Since ICRP66 assumed infinitely long airway tubes, the present work will study the DCC for tube lengths of 2 cm, which can then provide a direct comparison with the ICRP66 results.

1.1. Calculation of dose conversion coefficient according to ICRP66 model

The procedures for DCC calculation according to ICRP66 can be summarized as follows. (1) The first step is the calculation of the number of alpha particles, N_α, emitted for a given

exposure condition and time. This step requires computer programs to calculate deposition and clearance in various regions of the human respiratory tract (HRT). The results of these calculations will give an equilibrium activity of radon progeny in different regions of the HRT. From the equilibrium activity, the number of emitted alpha particles for a given period of time is determined. (2) The second step is the multiplication of N_α with the alpha-particle energy E_α and the AFs in targets, which gives the energy absorbed in the targets. The ratio between the energy absorbed and the mass of the targets gives the absorbed dose. In the ICRP66 model, the targets are layers containing the sensitive cells. (3) The third step involves weighting of the calculated doses as follows. First, the average dose in the BB region, D_{BB}, is found as

$$D_{BB} = 0.5D_{BB,bas} + 0.5D_{BB,sec} \quad (1)$$

where the same weighting factor 0.5 is employed for the dose $D_{BB,bas}$ in basal cells and the dose $D_{BB,sec}$ in secretory cells. Second, the doses in BB and bb are weighted by the factor 0.333 to give the dose in the tracheo-bronchial (T-B) tree, i.e.,

$$D_{T\text{-}B} = 0.333D_{BB} + 0.333D_{bb,sec} \quad (2)$$

The contribution to the total dose from the AI region is neglected here. (4) The fourth step calculates the effective dose as

$$E = 20 \times 0.12D_{T\text{-}B} \quad (3)$$

where 0.12 is a tissue weighting factor for the lung and 20 is a radiation weighting factor for alpha particles. The effective dose obtained by Eq. (3) is then divided by the corresponding potential alpha energy exposure (in the unit of WLM) employed above for the calculation of N_α, and finally the DCC (in the unit mSv/WLM) is obtained.

The DCC derived in this way is about 15 mSv/WLM and this is referred to as the dosimetric DCC value. In addition to the dosimetric value, there is a so-called epidemiologically derived DCC which is about 4 mSv/WLM. This large difference between the epidemiologically and dosimetrically derived DCC values has not been resolved until now. One of the proposals is to lower the value of the radiation weighting factor for alpha particles (Marsh et al., 2002; Hofmann et al., 2004; Stather, 2004).

2. Method

A home written program LUNGDOSE was applied to calculate the DCC values. Some programs like RADEP and LUDEP (Birchall et al., 1991; Jarvis and Birchall, 1994) are already available but they do not provide intermediate results that are required in our work. The program LUNGDOSE performed the following tasks:

(a) Calculate deposition of mono-dispersed aerosols in all regions of the HRT. The ICRP66 algebraic deposition model was implemented in the program.
(b) Summation according to three modes of lognormal distribution for the attached radon progeny to obtain total deposition in different regions.
(c) Implementation of the clearance model given in ICR66 to calculate equilibrium activities of radon progeny in all compartments of the HRT.
(d) Calculation of absorbed energies by multiplication of $N_\alpha E_\alpha$ with AF.
(e) Calculation of absorbed doses and the weighted values according to Eqs. (1)–(3).
(f) Determination of DCC.

Different parameters enter the dosimetric model of the HRT (Marsh and Birchall, 2000). If all of these parameters were kept at their best estimations, a DCC of 15 mSv/WLM was obtained by our LUNGDOSE program. The AFs used here were originally given in ICRP66 and they were related to the energy absorbed in the layers. Modifications made in the present work are as follows. The absorbed doses were calculated for the nuclei of sensitive cells. The nuclei of basal cells were approximated as cones while those for secretory cells as ellipsoids. Cylindrical geometry was adopted for the airway tubes as was proposed in ICRP66.

According to the ICRP66 model, basal cells exist only in the first eight generations of the HRT (BB region). In order to make simulations easier, the following simplified model was adopted. The origin was chosen at the bottom of a tube and the z-axis was along the tube axis, so the xOy plane was the same as the base of a tube. The cones representing the basal cells were distributed between two concentric cylinders with radii of R_1 and R_2 as proposed by ICRP66. The axes of all cones crossed the z-axis perpendicularly. The input parameter for these conical cells was the ratio between the cone height (H) and the cone radius (R), i.e., H/R. The parameter was chosen in such a way that the volume of the conical cell was the same as that for the spherical cells in previous investigations.

As regards the ellipsoidal secretory cells, the major axes of the ellipsoids were along lines that crossed the z-axis perpendicularly. The diameters of the nuclei of spherical secretory cells in BB were taken as 9 μm, cf. the radii $R_{sph} = 4.5$ μm (Hofmann et al., 2004). We also chose the nucleus volume of the ellipsoidal cells to be the same as those for spherical cells. The input parameter was the ratio between the major axis A_{ell} to R_{sph}. The abundance of basal and secretory cells was taken from Mercer et al. (1991).

Other elements of calculations were the same as those in our previous papers (Nikezic and Yu, 2001, 2003; Nikezic et al., 2003) and will not be repeated here in details. The difference was, as mentioned in Section 1, that long tubes with lengths of 2 cm were considered here instead of the 2 mm tubes considered in previous works.

3. Results

3.1. DCC calculations

The DCC was calculated for the following sets of the input parameters. The first set of parameters was related to the indoor room atmosphere: ventilation rate $\lambda_v = 0.55\ h^{-1}$; attachment rate $\lambda_a = 50\ h^{-1}$; deposition rate of unattached progeny $\lambda_d^u = 20\ h^{-1}$; deposition rate of attached progeny $\lambda_d^u = 0.20\ h^{-1}$; and recoil factor = 0.83. The attached progeny was assumed to distribute in three modes, namely, nucleation, accumulation and coarse modes, with the following fractions 0.28, 0.70 and 0.02, respectively (Nikezic and Stevanovic, 2004). These parameters were used in the Jacobi parametric room model, which then gave the ratios of progeny to radon concentration as shown in Table 1. These results were used as input data for the LUNGDOSE program. The total equilibrium factor was $F = 0.372$ and the unattached fraction was $f = 0.0655$. Other aerosol characteristics included: median diameters (with geometrical standard deviations in brackets) are 0.9 (1.3) nm, 50 (2) nm, 250 (2) nm and 1500 (1.5) nm for the unattached, nucleation, accumulation and coarse modes, respectively. The density of the

Table 1
Ratios of progeny to radon concentration in different modes for standard room conditions

Mode	^{218}Po/^{222}Rn	^{214}Pb/^{222}Rn	^{214}Po, ^{214}Bi/^{222}Rn
Unattached	0.162	0.014	0.000
Nucleation	0.158	0.100	0.076
Accumulation	0.394	0.251	0.190
Coarse	0.011	0.007	0.005

unattached progeny was taken as 1 g/cm^3, while that of the attached progeny as 1.4 g/cm^3; the shape factors taken as 1 and 1.1 for unattached and attached progeny, respectively; and hygroscopic growth factors as 1 and 1.5 for unattached and attached progeny, respectively.

The subject-related parameters were breathing rate = 0.78 m^3/h; tidal volume = 0.866 l/breath; functional residual capacity = 3300 ml; and breathing frequency = 15 min^{-1}. The half-life for transfer to blood was taken as 600 min. Other parameters that were not mentioned here were simply adopted as recommended in ICRP66. With these input parameters the equilibrium activities of radon progeny in different regions of the T-B tree were obtained and are shown in Table 2.

The equilibrium activities were further multiplied with the AFs of alpha-particle energy (given in ICRP66) and divided by the masses of the sensitive-cell layer to obtain the absorbed doses in different regions of the T-B tree per 1 WLM. Further weightings through Eqs. (1)–(3) were carried out and the final result was found as DCC = 15.05 mSv/WLM. This result is also given in Table 7.

3.2. Distribution of specific energy

The distribution of specific energy (Zaider and Rossi, 1986) with hit frequency was calculated for all combinations of different sources and targets. The distributions of specific energy (in the form of probability density) for different combinations of the sources, alpha energies and targets are shown in Figs. 1–3. Fig. 1 shows the distribution in conical basal cells with different ratios of H/R (i.e., 0.8, 1 and 1.2). Since the basal cells were close to the end of the range of 6 MeV alpha particles, it was relatively difficult to obtain good statistics in Monte Carlo calculations. No differences among the three graphs for $H/R = 0.8$, 1 and 1.2 were observed. The main characteristic of these graphs is the very large number of small energy transfer events for alpha particles with an initial energy of 6 MeV. The results for 7.69 MeV from slow and fast clearance mucus are almost overlapping. The case for 6 MeV alpha particles is different, where the results for the slow mucus are flatter than those for the fast mucus.

Fig. 2 gives the results for secretory cells in the BB region. Calculations were performed for three different ratios, viz., $A/R = 0.8$, 1 and 1.2, where A is the major axis of an ellipsoid and R is the radius of the sphere with the same volume as the ellipsoid. Two distinguishable peaks appear in each group of data, one on the left and one in the central part. The left peak is close to $z = 0$ and represents a relatively large number of events with very small energy transfer. The central peaks also appear in each group of the data and their locations depend on the energy as well as on the A/R ratio. The peak for 7.69 MeV alpha particles is around 0.3 Gy while that for 6 MeV alpha particles is around 0.4 Gy. When A/R increases, the peaks shift slightly to the right hand side.

Fig. 3 shows the data for the bb region. Here only secretory cells are present (according to ICRP66). Two groups of calculations were performed here for $A/R = 0.8$ and 1. Calculations

Table 2
Number of emitted alpha particles in different regions of the T-B tree

Source	Number of disintegration per 1 μm^3 of mucus/WLM	
	^{218}Po (6 MeV)	^{214}Po (7.69 MeV)
BB1 (fast mucus)	2.029×10^{-5}	6.979×10^{-5}
BB2 (slow mucus)	1.720×10^{-5}	6.260×10^{-5}
bb1 (fast mucus)	1.317×10^{-5}	8.924×10^{-5}
bb2 (slow mucus)	0.662×10^{-5}	4.784×10^{-5}

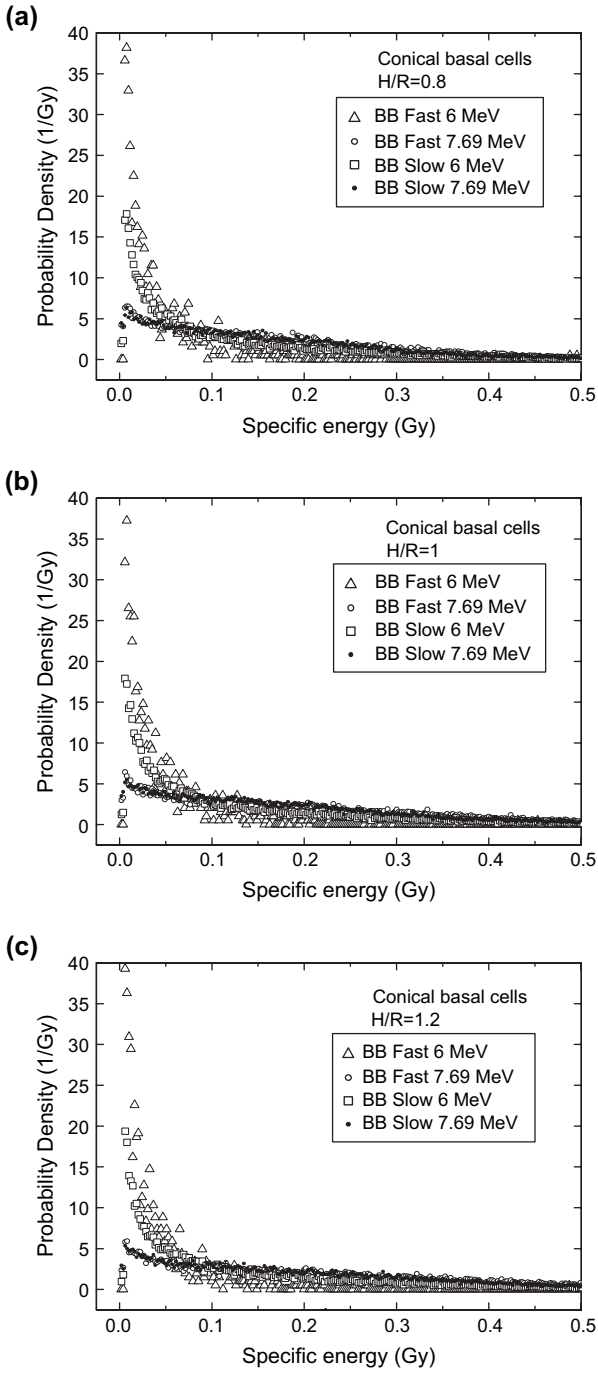

Fig. 1. Distribution of specific energy in conical basal cells: (a) for height to radius ratio = 0.8; (b) for height to radius ratio = 1; and (c) for height to radius = 1.2.

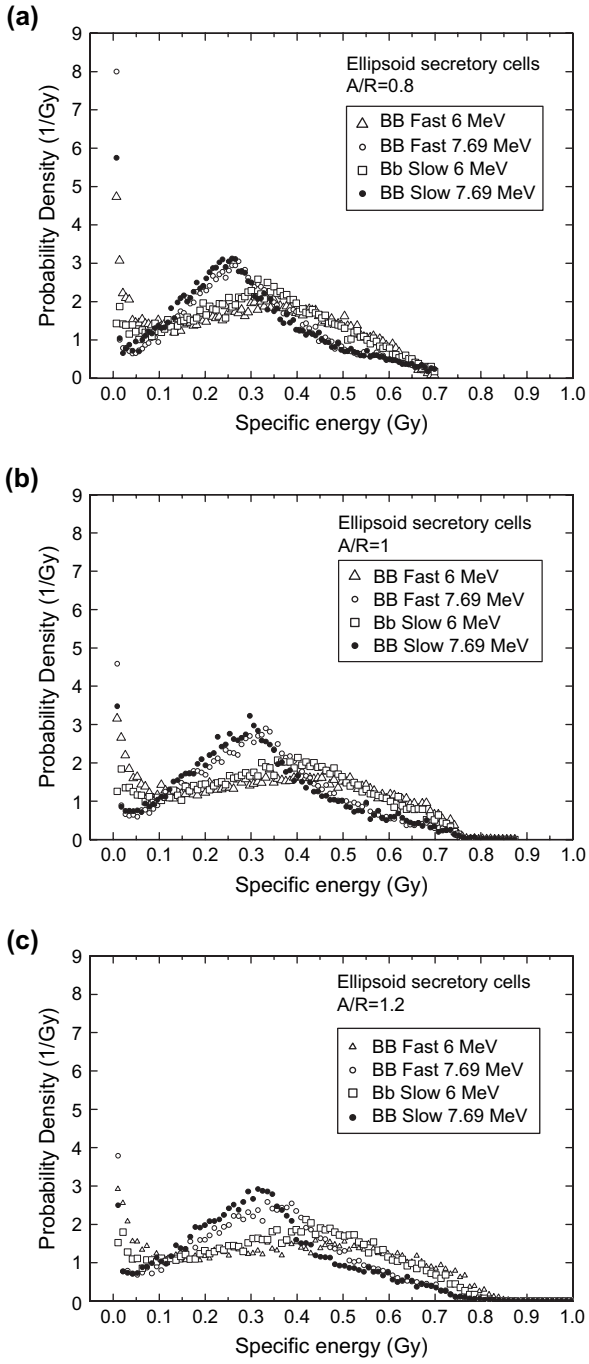

Fig. 2. Distribution of specific energy in secretory cells in the BB region: (a) for $A/R = 0.8$; (b) for $A/R = 1$; and (c) for $A/R = 1.2$.

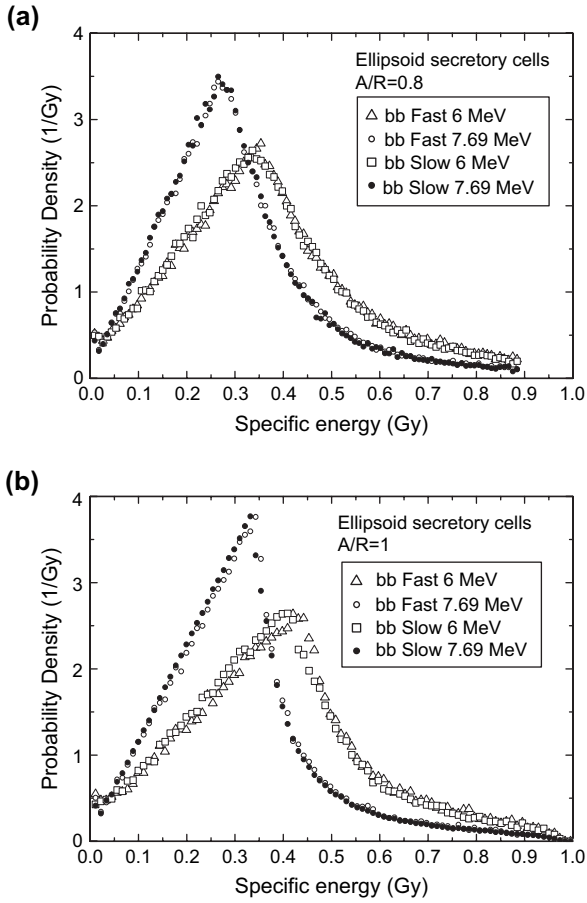

Fig. 3. Distribution of specific energy in secretory cells in the bb region: (a) for $A/R = 0.8$ and (b) for $A/R = 1$.

were not performed for $A/R = 1.2$ because part of such cell nuclei might be out of the layer defined by ICRP66. The layer containing the secretory-cell nuclei in the bb region was 8 μm thick. In our calculations, we just adopted that the spherical cell in this region had a radius of 4 μm. By taking $A/R = 1.2$, some parts of the nuclei would be out of the layer.

The simulation statistics was much better here because the target was close to the source, and a total of 10^6 hits were taken as the output criterion. For comparisons, the output criterion for secretory cells in the BB region was 10^5 hits and that for basal cells was 10^3 hits. Better statistics resulted in smaller scattering of data points in the figures. These curves show only one central peak; the left peak is missing or it is too low to recognize. These central peaks are more conspicuous for 7.69 MeV alpha particles than for 6 MeV alpha particles, and they also shift with increasing of A/R. There are no significant differences between the cases for alpha particle source in the fast and slow mucus, and the lines are almost overlapping.

3.3. Mean specific energy and dose conversion coefficient

From the graphs presented in Figs. 1–3, the mean specific energy $\bar{z}$ was calculated. The results are summarized in Tables 3–6. Tables 3–5 present the mean specific energy $\bar{z}$ and hit

Table 3
Specific energy ($\bar{z}$) and hit frequency (HF) in basal-cell nuclei in the BB (bronchial) region, which are considered as cones

Source	Energy (MeV)	*H*/*R*					
		0.8		1		1.2	
		$\bar{z}$ (Gy)	HF (WLM^{-1})	$\bar{z}$ (Gy)	HF (WLM^{-1})	$\bar{z}$ (Gy)	HF (WLM^{-1})
BB fast	6	0.064	1.02×10^{-5}	0.073	8.15×10^{-6}	0.064	6.73×10^{-6}
BB fast	7.69	0.154	0.011	0.181	8.72×10^{-3}	0.203	7.12×10^{-3}
BB slow	6	0.108	2.90×10^{-4}	0.116	2.45×10^{-4}	0.122	2.19×10^{-4}
BB slow	7.69	0.154	0.011	0.173	8.89×10^{-3}	0.195	7.82×10^{-3}

Three different ratios of cone height to cone radius (*H*/*R*) were used in the calculations. The cones have the same volume as spherical cells.

frequency (part of hit nuclei per exposure of 1 WLM) in basal cells in BB (Table 3), in secretory cells in BB (Table 4) and in secretory cells in bb (Table 5). The product of specific energy and hit frequency gives the absorbed dose *D* and the corresponding values in the unit mGy/WLM are given in Table 6.

The doses were weighted according to Eqs. (1)–(3) and the DCC in the unit mSv/WLM was also given in Table 7. Table 7 also gives the doses in layers that contain the basal- and secretory-cell nuclei and the corresponding DCC, which is actually the ICRP66 approach.

4. Discussion and conclusions

Distributions of specific energy were calculated for different combinations of alpha-particle sources, energies and targets. The distributions are shown in Figs. 1–3. The results for basal cells in the BB region show a large number of events per 1 Gy with very small energy transfer. Distributions of specific energy in secretory cells in the BB region have two peaks. Events with energy transfer around 0.3–0.4 Gy are frequent here and these are events with huge delivered dose. In the bb region, the distributions only have one peak.

The peaks for 7.69 MeV are on the left in comparison to the peaks of 6 MeV (in all graphs where central peak appear). Alpha particles with the initial energy of 7.69 MeV enter the sensitive-cell nuclei with larger energy than those particles with the initial energy of 6 MeV. The stopping power decreases with increasing energy, which results in the peak patterns as those observed in Figs. 1–3. All distributions have a long tail up to 1 Gy of specific energy.

Table 4
Specific energy ($\bar{z}$) and hit frequency (HF) in secretory-cell nuclei in the BB (bronchial) region, which are considered as ellipsoids

Source	Energy (MeV)	*A*/*R*					
		0.8		1		1.2	
		$\bar{z}$ (Gy)	HF (WLM^{-1})	$\bar{z}$ (Gy)	HF (WLM^{-1})	$\bar{z}$ (Gy)	HF (WLM^{-1})
BB fast	6	0.197	1.53×10^{-3}	0.340	1.38×10^{-3}	0.367	1.30×10^{-3}
BB fast	7.69	0.281	0.014	0.315	0.0128	0.330	0.013
BB slow	6	0.312	1.95×10^{-3}	0.345	1.76×10^{-3}	0.370	1.70×10^{-3}
BB slow	7.69	0.275	0.016	0.306	0.0146	0.317	0.014

Three different ratios of the major axis to the radius of sphere (*A*/*R*) with the same volume were used in the calculations.

Table 5
Specific energy ($\bar{z}$) and hit frequency (HF) in secretory-cell nuclei in the bb (bronchiolar) region, which are considered as ellipsoids

Source	Energy (MeV)	*A*/*R*			
		0.8		1	
		$\bar{z}$ (Gy)	HF (WLM^{-1})	$\bar{z}$ (Gy)	HF (WLM^{-1})
bb Fast	6	0.363	0.165×10^{-2}	0.388	0.160×10^{-2}
bb Fast	7.69	0.300	0.014	0.311	0.014
bb Slow	6	0.359	0.163×10^{-2}	0.380	0.167×10^{-2}
bb Slow	7.69	0.300	0.015	0.306	0.015

Two different ratios of major axis to the radius of sphere (*A*/*R*) with the same volume were used in calculation.

In Table 7, the data for DCC calculated in two different ways are presented. The DCC value obtained for cell nuclei is on average 13 mSv/WLM, which is less than the value obtained using the ICRP66 approach by 2 mSv/WLM. As described in Section 1, we previously obtained the DCC as 10 mSv/WLM by focusing on the spherical cell nuclei and by calculations for short airway tubes (2 mm) (Nikezic and Yu, 2001). To make direct comparisons with the ICRP66 results, which assumed infinitely long airway tubes, the present results have been obtained for long airway tubes (2 cm).

It is interesting to compare the results for different geometry for the cell nuclei obtained for long airway tubes. The values for spherical secretory-cell nuclei can be read from the values corresponding to $A/R = 1$, i.e., $D_{BB,sec} = 9.58$ mGy/WLM and $D_{bb} = 10.07$ mGy/WLM. However, the absorbed dose to spherical bronchial basal-cell nuclei $D_{BB,bas}$ should be recalculated, which is obtained as 4.12 mGy/WLM. Therefore, for spherical cell nuclei (and long airway tubes), the total DCC is calculated as 13.5 mSv/WLM. It can be seen that the absorbed dose to the bronchial basal-cell nuclei is significantly affected by their geometry. This is expected because basal cells are situated close to the end of the range of 6 MeV alpha particles. This also underlines the significance of better and more precise information on targets in the T-B tree.

One of the most critical issues is on the methodology in weighting the absorbed doses. The same weighting factor 0.5 is applied for the doses in the basal and secretory cells. In addition,

Table 6
Absorbed dose in cell nuclei in different regions of the T-B tree

Source	Energy (MeV)	Target	(*H*/*R*) or (*A*/*R*)		
			0.8	1	1.2
			Absorbed dose mGy/WLM		
BB fast	6	Secretory	0.301	0.469	0.477
BB fast	7.69	Secretory	4.018	4.032	4.124
BB slow	6	Secretory	0.608	0.607	0.629
BB slow	7.69	Secretory	4.318	4.468	4.470
BB fast	6	Basal	6.6×10^{-4}	5.9×10^{-4}	4.3×10^{-4}
BB fast	7.69	Basal	1.632	1.578	1.446
BB slow	6	Basal	3.1×10^{-2}	2.9×10^{-2}	2.7×10^{-2}
BB slow	7.69	Basal	1.756	1.538	1.525
bb Fast	6	Secretory	0.599	0.620	–
bb Fast	7.69	Secretory	4.169	4.255	–
bb Slow	6	Secretory	0.584	0.634	–
bb Slow	7.69	Secretory	4.478	4.560	–

Table 7
The Absorbed dose (mGy/WLM) and the total DCC (mSv/WLM) calculated for layers that contain the basal- and secretory-cell nuclei (ICRP66 approach) and for the cell nuclei themselves (approach used in the present work)

	Layers	Cell nuclei (different H/R or A/R)		
		0.8	1	1.2
Absorbed dose (mGy/WLM)				
Bronchial basal cells, $D_{BB,bas}$	5.15	3.42	3.15	3.00
Bronchial secretory cells $D_{BB,sec}$	11.69	9.25	9.58	9.70
Bronchial dose ($0.5D_{BB,bas} + 0.5D_{BB,sec}$)	8.42	6.33	6.36	6.35
Bronchiolar D_{bb}	10.42	9.83	10.07	–
Total DCC (mSv/WLM)	15.05	12.92	13.13	13.12

the same weighting factor 0.333 is applied to sum the doses in the BB and bb regions. If one applies 0.8 and 0.2 to weight the basal and secretory cells, respectively, and 0.4 and 0.266 to weight D_{BB} and D_{bb}, DCC $\cong$ 10.6 mSv/WLM is obtained. This value is close to the newest epidemiological results. USEPA (2003) gave the risk estimate as 5.38×10^{-4} fatal lung cancers per WLM. This value was divided by the detriment per Sv given by ICRP (1990), i.e., 5.6×10^{-2} per Sv, to give the DCC. Therefore, for the new risk estimate suggested by USEPA, the corresponding DCC was about 9.6 mSv/WLM.

Acknowledgment

The present research is supported by the CERG grant CityU 103204 from the Research Grant Council of Hong Kong.

References

Birchall, A., Bailey, M.R., James, A.C., 1991. LUDEP: a lung dose evaluation program. Radiation Protection Dosimetry 38, 167–174.

Hofmann, W., Fakir, H., Aubineau-Laniece, I., Pihet, P., 2004. Interaction of alpha particles at the cellular level – implications for the radiation weighting factor. Radiation Protection Dosimetry 112, 493–500.

ICRP, 1990. ICRP Publication 60. Recommendations of the International Commission on Radiological Protection. Pergamon Press, Oxford.

ICRP, 1994. ICRP Publication 66. Human Respiratory Model for Radiological Protection. A Report of a Task Group the International Commission on Radiological Protection. Pergamon Press, Oxford.

Jarvis, N.S., Birchall, A., 1994. LUDEP 1.0, a personal computer program to implement the new ICRP respiratory tract model. Radiation Protection Dosimetry 53, 191–193.

Marsh, J.W., Birchall, A., 2000. Sensitivity analysis of the weighted equivalent lung dose per unit exposure from radon progeny. Radiation Protection Dosimetry 87, 167–178.

Marsh, J.W., Birchall, A., Butterweck, G., Dorrian, M.-D., Huet, C., Ortega, X., Reineking, A., Tymen, G., Schuler, C.H., Vargas, A., Vessu, G., Wendt, J., 2002. Uncertainty analysis of the weighted equivalent lung dose per unit exposure to radon progeny in the home. Radiation Protection Dosimetry 102, 229–248.

Mercer, R.R., Russel, M.L., Crapo, J.D., 1991. Radon dosimetry based on the depth distribution of nuclei in human and rat lungs. Health Physics 61, 117–130.

Nikezic, D., Yu, K.N., 2001. Microdosimetric calculation of absorption fraction and the resulting dose conversion factor for radon progeny. Radiation and Environmental Biophysics 40, 207–211.

Nikezic, D., Yu, K.N., 2003. Absorbed fraction of alpha particles emitted in bifurcation regions of the human tracheobronchial tree. Radiation and Environmental Biophysics 42, 49–53.

Nikezic, D., Novakovic, B., Yu, K.N., 2003. Absorbed fraction of radon progeny in human bronchial airways with the bifurcation geometry. International Journal of Radiation Biology 79, 175–180.

Nikezic, D., Stevanovic, N., 2004. Room model with three modal distributions of attached radon progeny. Health Physics 87, 405–409.

Stather, J.W., 2004. Dosimetric and epidemiological approaches to assessing radon doses – can the differences be reconciled? Radiation Protection Dosimetry 112, 487–492.

USEPA, United States Environmental Protection Agency, 2003. EPA Assessment of Risks from Radon in Homes. Office of Radiation and Indoor Air, Washington, DC.

Zaider, M., Rossi, H., 1986. Microdosimetry and its application to biological processes. In: Orton, Colin G. (Ed.), Radiation Dosimetry. Plenum Press, New York, pp. 171–242.